

Description of shape coexistence in  $^{96}\text{Zr}$  based on the quadrupole-collective Bohr HamiltonianD. A. Sazonov,<sup>1,2</sup> E. A. Kolganova,<sup>1,2</sup> T. M. Shneidman,<sup>1,3</sup> R. V. Jolos,<sup>1,2</sup> N. Pietralla,<sup>4</sup> and W. Witt<sup>4</sup><sup>1</sup>Joint Institute for Nuclear Research, 141980 Dubna, Moscow Region, Russia<sup>2</sup>Dubna State University, 141982 Dubna, Moscow Region, Russia<sup>3</sup>Kazan Federal University, Kazan 420008, Russia<sup>4</sup>Institut für Kernphysik, TU Darmstadt, Schlossgartenstrasse 9, D-64289 Darmstadt, Germany

(Received 9 January 2019; revised manuscript received 4 February 2019; published 18 March 2019)

Experimental data on  $^{96}\text{Zr}$  indicate coexisting spherical and deformed structures with small mixing amplitudes. Although a possible geometrical description of such a shape coexistence is implied in the contemporary discussion, it does not exist yet for  $^{96}\text{Zr}$ . The observed properties of the low-lying collective states of  $^{96}\text{Zr}$  based on the geometrical collective model are investigated. The quadrupole-collective Bohr Hamiltonian with the potential having two minima, spherical and deformed, is applied. Good agreement with the experimental data on the excitation energies,  $B(E2)$ , and  $B(M1)$  reduced transition probabilities is obtained. It is shown that the low-energy structure of  $^{96}\text{Zr}$  can be described in a satisfactory way within the geometrical collective model with a potential function supporting shape coexistence without other restrictions of its shape. However, the excitation energy of the  $2_2^+$  state can be reproduced only if the rotation inertia coefficient is taken to be 5 times smaller than the vibrational one in the region of the deformed well. It is shown also that shell effects are important for the description of  $B(M1; 2_2^+ \rightarrow 2_1^+)$ . An indication of the influence of the pairing vibrational mode on the  $0_2^+ \rightarrow 0_1^+$  transition is obtained.

DOI: [10.1103/PhysRevC.99.031304](https://doi.org/10.1103/PhysRevC.99.031304)

Shape coexistence in nuclei is a remarkable phenomenon which has become a widespread feature that may occur in many nuclei. The occurrence of different shapes has its origin in the evolution of shell structure with excitation energy and varying occupation of nucleonic orbitals [1–3]. It was discussed in Ref. [4] that the occurrence of the shape coexistence can be related to the existence of a sufficiently large energy gap between subshells. Closely spaced subshells lose their individuality due to pairing correlations and behave as a single, large subshell supporting deformation. In the presence of the well-defined subshells in the spherical single-particle level scheme a strong redistribution of nucleons over the single-particle levels can take place by particle-hole transitions with increasing excitation energy. This helps to stabilize the deformation of the excited states when the ground state is spherical [5]. A substantial change of a configuration of nucleons may lead to a large difference in microscopic structure between the spherical states and the states with deformation-optimized shell structure. This property can decrease the mixing of two configurations of different shapes. Although the explanation of shape coexistence phenomena is a subject of microscopic nuclear models, the collective model treats directly the shape parameters as its dynamical variables and, thus, is supposed to describe the dynamical consequences of shape coexistence in a simple way.

The basic idea of the nuclear collective model is that, even though such a quantum many-body system as the atomic nucleus is characterized by a huge amount of microscopic degrees of freedom, they are organized in collective modes playing a crucial role in determining nuclear structure.

Consequently, a collective Hamiltonian can be constructed which includes, in the case of the geometrical collective model, as the basic ingredients the deformation-dependent collective potential and the tensor of inertia [6,7]. This Hamiltonian determines nuclear collective dynamics.

A shape evolution of the nuclear states can happen as a function of excitation energy, angular momentum, and the number of nucleons. The shape transition with the number of nucleons has been noticed in many chains of isotopes and isotones but appears to be rather gradual in many cases. The abrupt change of shape in Zr isotopes [8–10] is exceptional. This is a notable feature of nuclear structure in  $A \approx 100$  nuclei. The structure of Zr isotopes has been studied within the framework of many different models [11–24]. Strongly deformed states coexisting with a nearly spherical ground state have been reported for Sr and Zr isotopes [25–27]. In parallel with a smooth or abrupt establishment of a deformed shape, a significant mixing between the configurations of a different shape or a suppressed mixing of two such configurations can be considered. Such information can be obtained from electromagnetic transition probabilities. By measuring the electromagnetic decay properties of the collective  $2_2^+$  state of  $^{96}\text{Zr}$  [28] the high purity of the coexisting states has recently been established. Some low-lying excited states of  $^{96}\text{Zr}$  are related by strong  $E2$  transitions. Therefore, it is natural to consider them in the framework of the collective quadrupole model with a Bohr Hamiltonian and it is intriguing to study to what extent the collective model is capable of reproducing the experimentally observed situation. The interpretation of the observed properties of  $^{96}\text{Zr}$  in the framework of the

geometrical collective model is, thus, an important task and it is the main motivation to undertake the present investigation. In Refs. [5] and [28] the properties of  $^{96}\text{Zr}$  have been considered in the framework of the shell model.

An explanation of the observed high purity of the co-existing spherical and deformed states in the framework of the geometrical collective model requires a consideration of the collective Hamiltonian having a potential with two minima. To our knowledge the Bohr Hamiltonian with such potential has been considered up to now only in the papers of two groups [29–32] where the sextic-type potential has been treated with quite restricted possibilities for variation of the relative depth of the spherical and deformed minima, a rigidity of the potential near the minima, and a height and width of the barrier separating two minima. However, in order to verify a principal possibility of the description of the observed properties of  $^{96}\text{Zr}$  within the geometrical collective model it is important to consider a potential with spherical and deformed minima, however, without any other restrictions of their shapes, i.e., including shallow regions around the minima for the occurrence of soft deformation. In the present paper the experimental data for  $^{96}\text{Zr}$  are analyzed based on the  $\beta$ -dependent potential with two minima separated by a barrier; however, all other characteristics of the potential, e.g., relative depth of two minima, the height and width of the barrier, and other characteristics of the potential, are varied without restrictions so as to achieve a satisfactory description of the observed properties of the low-lying states of  $^{96}\text{Zr}$ .

Thus, the aim of the present paper is to investigate an option to approximately describe, in principle, the properties of the low-lying collective  $0_{1,2}^+$  and  $2_{1,2}^+$  states of  $^{96}\text{Zr}$  and a weak mixing of the configurations characterized by spherical and deformed shapes based on the quadrupole-collective Bohr Hamiltonian. At the end of the paper we consider briefly the characteristics of the  $4_1^+$  and  $0_3^+$  states. It is also interesting how the impact of shell effects are manifested in such a description.

The quadrupole-collective Bohr Hamiltonian takes the form [33]

$$H = -\frac{\hbar^2}{2B_0} \frac{1}{\sqrt{wr}} \frac{1}{\beta^4} \frac{\partial}{\partial \beta} \beta^4 \sqrt{\frac{r}{w}} b_{\gamma\gamma} \frac{\partial}{\partial \beta} + \hat{T}_{\beta\gamma} + \hat{T}_\gamma + \frac{\hbar}{2B_0} \sum_{\kappa} \frac{\hat{I}_{\kappa}^2}{\mathfrak{S}_{\kappa}} + V(\beta). \quad (1)$$

The first term in Eq. (1) presents the kinetic energy of  $\beta$  vibrations. The second and the third terms are connected to the  $\gamma$  degrees of freedom. The last two terms are the rotational and potential energies. Above,

$$w = b_{\beta\beta} b_{\gamma\gamma} - b_{\beta\gamma}^2, \quad r = b_1 b_2 b_3, \quad (2)$$

$$\mathfrak{S}_{\kappa} = 4b_{\kappa} \beta^2 \sin^2 \left( \gamma - \frac{2\kappa\pi}{3} \right).$$

The parameter  $B_0$  is a dimensional scaling factor for the components of the inertia tensor. Thus, the coefficients  $b_{\beta\beta}$ ,  $b_{\gamma\gamma}$ ,  $b_{\beta\gamma}$ , and  $b_{\kappa}$  are dimensionless inertia coefficients for the  $\beta$  and  $\gamma$  vibrations and the rotational motion. The collective potential is determined below.

TABLE I. The results of calculations of the energies and electromagnetic reduced transition probabilities for  $^{96}\text{Zr}$ . The value of  $b_{\text{rot}}$  is taken as 0.2. The values of  $B(E2)$  are given in Weisskopf units and those of  $B(M1)$  are given in nuclear magnetons. The value of  $Q(2_2^+)$  is given in  $e$  b. The excitation energies are given in keV. The experimental energy of the  $0_2^+$  state is used to fix the value of  $B_0$ . Experimental data are taken from Refs. [28,39].

Energies and transitions	Calc.	Expt.
$E(2_1^+)$	1748	1750
$E(2_2^+)$	2268	2226
$E(0_2^+)$	1582*	1582
$B(E2; 2_2^+ \rightarrow 0_2^+)$	26.1	36(11)
$B(E2; 2_1^+ \rightarrow 0_1^+)$	3.6	2.3(3)
$B(E2; 2_2^+ \rightarrow 0_1^+)$	0.26	0.26(8)
$\rho^2(0_2^+ \rightarrow 0_1^+)$	0.0013	0.0075
$B(E2; 2_2^+ \rightarrow 2_1^+)$	2.25	$2.8_{-1.0}^{+1.5}$
$B(E2; 2_1^+ \rightarrow 0_2^+)$	6.8	—
$B(M1; 2_2^+ \rightarrow 2_1^+)$	0.11	0.14(5)
$Q(2_2^+)$	-0.51	—

For keeping our task at a manageable size we assume that the  $\gamma$  degrees of freedom can be separated from  $\beta$  in the potential and the value of  $\gamma$  is stabilized around  $\gamma = 0$ . We mention, however, that the results for the potential energy surface of  $^{96}\text{Zr}$  presented in Ref. [28] rather indicate a triaxial shape in its  $2_2^+$  and  $0_2^+$  states. Triaxiality should decrease significantly the result presented in Table I for  $Q(2_2^+)$ . Thus, future experimental data on this quantity will give us information on the shape of  $^{96}\text{Zr}$ .

A separation of  $\beta$  and  $\gamma$  in the potential is not sufficient for the complete separation of  $\beta$  and  $\gamma$  degrees of freedom since they are coupled through the kinetic energy term. However, this coupling effectively produces an additional  $\sim 1/\beta^2$  type term in  $V(\beta)$  [34]. Thus, the potential obtained below fitting the data includes, in fact, the effect of the  $\beta$ - $\gamma$  coupling through the kinetic energy term. It is found in our calculations that the interpretation of the existing experimental data on  $0_{1,2}^+$  and  $2_{1,2}^+$  states does not require an introduction of a  $\beta$ -dependent  $b_{\beta\beta}$  coefficient. Thus, we put below  $b_{\beta\beta} = 1$ . We assume also, for simplicity, that  $b_1 = b_2 = b_3 \equiv b_{\text{rot}}$ .

After approximations discussed above we obtain the following expression for the collective Hamiltonian:

$$H = -\frac{\hbar^2}{2B_0} \frac{1}{b_{\text{rot}}^{3/2}} \frac{1}{\beta^4} \frac{\partial}{\partial \beta} \beta^4 b_{\text{rot}}^{3/2} \frac{\partial}{\partial \beta} + \frac{\hbar^2}{2B_0} \frac{\hat{I}^2 - \hat{I}_3^2}{3b_{\text{rot}}\beta^2} + V(\beta). \quad (3)$$

A description of the  $\beta$  motion only, without consideration of the  $\gamma$  variable, was realized for the first time in the Davydov-Chaban model [35]. It was assumed there that  $\gamma$  is a constant and not a collective variable. Thus, a collective motion has been considered not in the five-dimensional but in the four-dimensional space. As a result,  $\beta^3$  was presented instead of  $\beta^4$  in the kinetic energy term of the  $\beta$  motion. Having in mind a future generalization of our consideration to the full  $\beta$ - $\gamma$  plane we treat  $\gamma$  as a collective variable, however, separated from  $\beta$  (see, for instance, Ref. [36]).

Using the Hamiltonian (3) to obtain an equation for the collective wave function and excluding from this equation a term with a first derivative over  $\beta$  we get the Schrödinger equation in the following form:

$$\left\{ -\frac{\hbar^2}{2B_0} \frac{d^2}{d\beta^2} + \frac{\hbar^2}{2B_0} \frac{\hat{I}^2 - \hat{I}_3^2}{3b_{\text{rot}}\beta^2} + V(\beta) + \frac{\hbar^2}{2B_0} \left[ \frac{1}{4\tau} \frac{d^2\tau}{d\beta^2} - \frac{3}{16} \left( \frac{1}{\tau} \frac{d\tau}{d\beta} \right)^2 \right] \right\} \Phi = E\Phi, \quad (4)$$

where  $\tau = \beta^8 b_{\text{rot}}^3$ . We keep in Eq. (4) the rotational inertia coefficient because, as it was found in Refs. [37,38], in the case of well-deformed axially symmetric nuclei the inertia coefficient for the rotational motion is 4–10 times smaller than the inertia coefficient for the vibrational motion. In a complete correspondence with this result it is shown below that in order to explain the excitation energy of the  $2_2^+$  state it is necessary to take  $b_{\text{rot}}/b_{\beta\beta}$  several times less than unity.

Using the wave functions from Eq. (4) the matrix elements of an arbitrary operator  $\hat{F}$  are calculated as

$$\langle i|\hat{F}|j\rangle = \int_0^\infty d\beta \Phi_i^* \hat{F} \Phi_j. \quad (5)$$

The  $E2$  reduced transition probability is given by the following expression:

$$B(E2; I_i \rightarrow I_f) = \left( \frac{3}{4\pi} Z e R_0^2 \right)^2 (C_{I_i 0 20}^{I_f 0})^2 |\langle i|\beta|j\rangle|^2, \quad (6)$$

where  $R_0$  is the nuclear radius and  $C_{I_i 0 20}^{I_f 0}$  is the Clebsch-Gordan coefficient. The  $E0$  transition strength  $\rho^2(E0; I_i \rightarrow I_f)$ , which is defined as  $\rho^2(E0; i \rightarrow f) \equiv |\langle f|M(E0)|i\rangle|^2 / (eR_0^2)^2$ , and in the collective model  $M(E0) = 3/4\pi Z e R_0^2 \beta^2$ , is given by

$$\rho^2(0_2^+ \rightarrow 0_1^+) = \left( \frac{3}{4\pi} Z \right)^2 |\langle 0_2^+|\beta^2|0_1^+\rangle|^2. \quad (7)$$

The  $M1$  reduced transition probability is calculated assuming the following expression for the  $M1$  transition operator:

$$(M1)_\mu = \mu_N \sqrt{\frac{3}{4\pi}} g_R(\beta) \hat{I}_\mu, \quad (8)$$

where  $\mu_N$  is the nuclear magneton and  $g_R(\beta)$  is the deformation-dependent collective  $g$  factor. This form of the  $M1$  transition operator is justified below. Thus,

$$B(M1; 2_2^+ \rightarrow 2_1^+) = \mu_N^2 \frac{9}{2\pi} |\langle 2_2^+|g_R(\beta)|2_1^+\rangle|^2. \quad (9)$$

The Hamiltonian (4) contains two important ingredients that determine the results of our calculations: the potential energy as a function of  $\beta$  and the inertia coefficient for the rotational motion. To describe the shape of the potential we defined several points fixing the positions of the spherical and deformed minima, the rigidity of the potential near its minima, and the height and width of the barrier separating the two minima. The deformation at the second minimum has been taken to be  $\beta = 0.24$  in agreement with the experimental value of  $B(E2; 2_2^+ \rightarrow 0_2^+)$ . The potential energy as a function

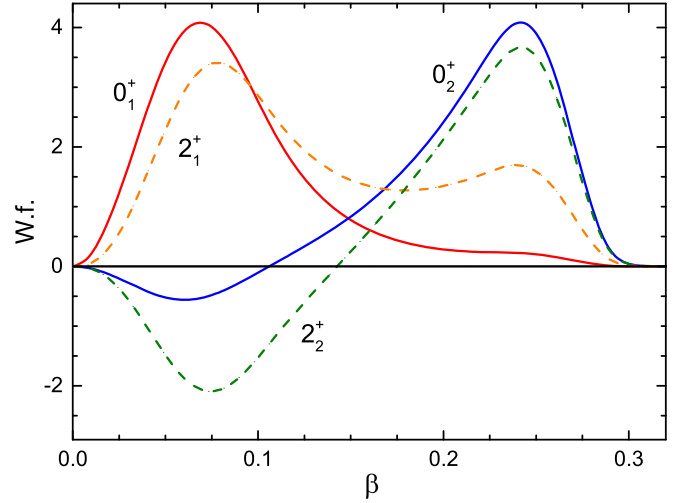


FIG. 1. The wave functions of the  $0_1^+$ ,  $0_2^+$ ,  $2_1^+$ , and  $2_2^+$  states.

of  $\beta$  is determined by using cubic spline interpolation between selected points. Then we numerically solve the Schrödinger equation (4) with zero boundary conditions, varying selected points in order to get a satisfactory description of the energies of the  $2_1^+$  and  $2_2^+$  states and the following transition probabilities:  $B(E2; 2_2^+ \rightarrow 0_2^+)$ ,  $B(E2; 2_1^+ \rightarrow 0_1^+)$ , and  $B(E2; 2_2^+ \rightarrow 0_1^+)$ . The number of points is taken to be between 10 and 13, although we did not aim at a minimization of the number of points determining the shape of the potential. Small variations of the positions of some points can lead to noticeable variations of the values of observables. The parameter  $B_0$  has been varied to fix the energy of the  $0_2^+$  state.

We have initially assumed that the rotational inertia coefficient  $b_{\text{rot}} = 1$ . It was found in this case that the main problem for describing the experimental data is related to the reproduction of the excitation energy of the  $2_2^+$  state together with the  $0_2^+$  state. This energy spacing was obtained at several hundreds of keV lower than the experimental value. As it is shown in Fig. 1 the wave function of the  $2_2^+$  state is located in the deformed well of the potential. Therefore, this state can be interpreted qualitatively as a rotational state based on the  $0_2^+$  state, and its energy is determined by the deformation at the minimum of the deformed well and the rotational inertia coefficient. The deformation at the minimum of the deformed well is related to the  $B(E2; 2_2^+ \rightarrow 0_2^+)$  value. Therefore, the calculated value of the excitation energy of the  $2_2^+$  state can be improved only if we assume that the rotational inertia coefficient  $b_{\text{rot}}$  is smaller than the vibrational inertia coefficient, i.e., that  $b_{\text{rot}}/b_{\beta\beta} < 1$ .

The results for the energies of the low-lying collective states and the electromagnetic transition probabilities obtained, assuming that the rotational inertia coefficient is 5 times smaller than the vibrational one (i.e.,  $b_{\text{rot}} = 0.2$ ), are shown in Table I and in Fig. 2.

The results presented in Table I are obtained assuming that  $\gamma = 0$ . This assumption does not influence the results for  $B(E2; 2_1^+ \rightarrow 0_1^+)$ . However, in the case of  $\gamma = 30^\circ$ ,  $Q(2_2^+) = 0$ . As it is seen from the results presented in Table I the agreement between the calculated results and the

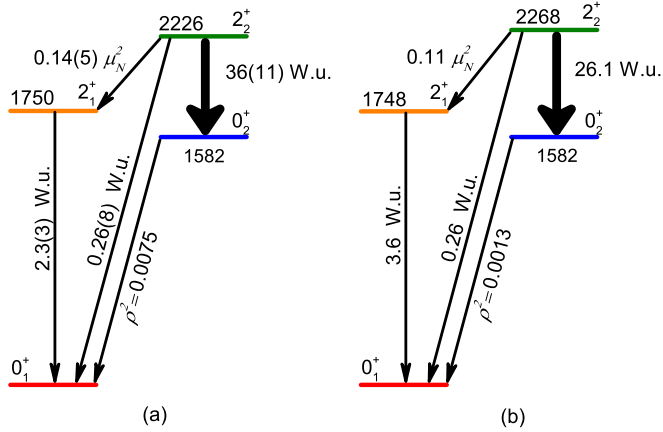


FIG. 2. Experimental (a) and calculated (b) low-lying  $0^+$  and  $2^+$  states of  $^{96}\text{Zr}$ . Excitation energies are given in keV. The values of electric transition probabilities are given in Weisskopf units and those of magnetic ones are in nuclear magnetons. Experimental data are taken from Ref. [28].

experimental data is satisfactory. The results for  $\rho^2(0_2^+ \rightarrow 0_1^+)$  and  $B(M1; 2_2^+ \rightarrow 2_1^+)$  are discussed below. The value of  $\rho^2(0_2^+ \rightarrow 0_1^+)$  is a factor 3.6 smaller than the experimental value. However, both the experimental and the calculated  $\rho^2(0_2^+ \rightarrow 0_1^+)$  values are small in comparison to the corresponding quantities in other nuclei [40].

Taking the average of a double commutator  $[[H, \beta^2], \beta^2] = (4\hbar^2/B_0)\beta^2$  over the ground state and using the well-known relation between  $\langle 0_1^+ | \beta^2 | 0_1^+ \rangle$  and  $B(E2; 2_1^+ \rightarrow 0_1^+)$  [41], we can derive the following relation:

$$\rho^2(0_2^+ \rightarrow 0_1^+) \leq \frac{\hbar^2}{B_0} \frac{1}{E(0_2^+)} \frac{10B(E2; 2_1^+ \rightarrow 0_1^+)}{e^2 R^4}. \quad (10)$$

In our calculations the value of  $\hbar^2/B_0$  was fixed as 8.062 keV to reproduce the experimental value of  $E(0_2^+)$ . Substituting this value and the experimental values of  $E(0_2^+)$  and  $B(E2; 2_1^+ \rightarrow 0_1^+)$  into Eq. (10) we obtain that  $\rho^2(0_2^+ \rightarrow 0_1^+) \leq 0.0035$ , in satisfactory correspondence to the result given in Table I.

This result means that we can reproduce the experimental value of  $\rho^2(0_2^+ \rightarrow 0_1^+) = 0.0075$  using the collective model with quadrupole degrees of freedom only within a factor of 2. We cannot exclude that the pairing vibrational mode plays an important role in a description of the  $E0$  transitions [42].

Consider now the result obtained for the  $B(M1; 2_2^+ \rightarrow 2_1^+)$  value. Application of the collective model expression for the  $M1$  transition operator [43] gives a value that is more than 3 orders smaller than the experimental one. This means that another approach should be used to derive an expression for the  $M1$  operator. In this rapid communication we only indicate a way in which this can be done. The expression for the  $M1$  transition operator suitable for use within the geometrical collective model can be obtained in the framework of the generator coordinate method. Qualitatively, we can suggest the following procedure; however, a detailed presentation of the derivation of the required expression needs a separate

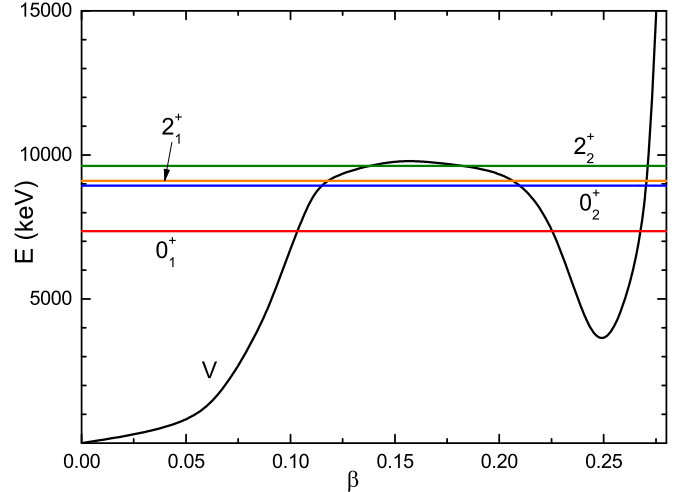


FIG. 3. The potential energy  $V(\beta)$  and the calculated energy levels.

publication. After some approximations described in Ref. [44] (see also Ref. [45] where the expression for the arbitrary single-particle operator has been derived), the final expression looks to be a product of the geometrical factor reflecting the dipole character of the  $M1$  transition operator and an integral over  $\beta$ . This integral is a product of the diagonal matrix element of the  $M1$  single-particle operator, taken over the BCS wave function obtained for the given value of  $\beta$ , and the collective wave functions of the initial and final states. This expression looks like the integral in Eq. (9). Thus, the matrix element mentioned above can be identified with  $g_R(\beta)$ . At  $\beta = 0$  it is natural to take this matrix element to be equal to the shell model value of the  $g$  factor of the  $2_1^+$  state, namely,  $-0.26$ . We assume this value to be correct inside the spherical well. In the deformed well we can use the standard collective model value  $Z/A$ . The calculations of the collective  $g$  factor for the well-deformed nuclei [46] indeed always gives a positive value close to  $Z/A$ ; however, this value can differ for neighboring isotopes and is usually smaller than  $Z/A$ . Then we interpolate between these two values assuming a narrow transition region in  $\beta$  where the wave function of the  $2_2^+$  state changes its sign.

With this transition operator we obtain  $B(M1; 2_2^+ \rightarrow 2_1^+) = 0.11\mu_N^2$ , which coincides in the limit of the experimental uncertainties with the experimental value  $0.14\mu_N^2$  [28]. This result stresses the importance of the shell effects for the description of the shape coexistence phenomena, at least, in the case of  $^{96}\text{Zr}$ .

The collective potential, which has been fixed phenomenologically to describe the experimental data, is shown in Fig. 3. The height of the barrier calculated from the energy of the ground state is equal to 2.45 MeV.

The wave functions of the ground and excited states are shown in Fig. 1. Their distribution between the spherical and deformed parts of the total potential is characterized by the values obtained by integration of the squares of the wave functions over the regions inside the spherical or deformed wells. These values are presented in Table II.

TABLE II. Distribution of the wave function of the  $0_1^+$ ,  $0_2^+$ ,  $2_1^+$ , and  $2_2^+$  states between the spherical and deformed parts of the total potential.

Potential well	$0_1^+$	$0_2^+$	$2_1^+$	$2_2^+$
Spherical	98.9%	3.2%	77.3%	23.7%
Deformed	1.1%	96.8%	22.7%	76.3%

As the value of  $\beta$  separating the spherical and deformed wells we have considered several points: the zeros of the  $2_2^+$  and  $0_2^+$  wave functions, and the middle of the barrier. The results obtained are not very sensitive to this choice. As we see from Table II the wave function of the  $I^\pi = 0_{1,2}^+$  states are practically concentrated in one well: spherical for the  $0_1^+$  state and deformed for the  $0_2^+$  state [23,28]. Qualitatively the same situation is realized in the case of the  $I^\pi = 2_{1,2}^+$  states. However, in this case the distribution of the wave functions between the spherical and deformed wells is less asymmetric. As it is seen from Table II the wave function of the  $2_1^+$  state is also located mainly in the spherical well like the  $0_1^+$  state. However, its weight in the deformed minimum is equal to 22.7%, i.e., significantly larger than for the  $0_1^+$  state.

In addition to the states considered above there are the  $4_1^+$  state, which decays by a strong  $E2$  transition to the  $2_2^+$  state, and the  $0_3^+$  state, also decaying to the  $2_2^+$  state by a strong  $E2$  transition. This means that both the  $4_1^+$  and  $0_3^+$  states can be considered in the model presented in this rapid communication. Our preliminary calculations with the potential fitted above have shown that the wave function of the  $4_1^+$  state is concentrated in the deformed well. Therefore, this state can be considered as a member of the band including the  $0_2^+$  and  $2_2^+$  states. However, we have obtained that the ratio  $[E(4_1^+) - E(0_2^+)]/[E(2_2^+) - E(0_2^+)]$  is equal to 2.5. This value is much lower than the typical rotational ratio of 3.33; however, is larger than the experimental value of 2.0. The reason for this result is the closeness of the energy of the  $4_1^+$  state to the barrier height.

As we have found in our calculations the height of the barrier can be varied in some limits without significant changes of the results obtained for the  $0_{1,2}^+$  and  $2_{1,2}^+$  states, including

an extent of localization of these states in the spherical and deformed wells. Of course, some values are changed; however, an overall agreement with experimental data remains. Thus, inclusion of the higher excited states into consideration can demand a change of the height of the barrier, since these states are lying above the barrier, and the form of the potential at deformations larger than  $\beta = 0.24$ . At the same time, the noncollective degrees of freedom increase with excitation energy and start to play an important role. This will limit the possibility of the description of the experimental data within the collective model.

For the energy of the  $0_3^+$  state we obtained a value that is much larger than the experimental one. Probably, this means that the structure of the  $0_3^+$  state is related to the excitation of the  $\gamma$  mode.

In conclusion, we have studied a possibility to describe the properties of the low-lying collective states of  $^{96}\text{Zr}$  based on the quadrupole-collective Bohr Hamiltonian in terms of axially symmetric shape coexistence. The potential energy of this Hamiltonian is fixed to describe the experimental data in a satisfactory way. This potential has two minima—spherical and deformed separated by a barrier. Good agreement with the experimental data is obtained for the excitation energies,  $B(E2)$ , and  $B(M1)$  values of the lowest-lying states. It is shown that the experimental value of the excitation energy of the  $2_2^+$  state can be reproduced only if the rotational inertia coefficient in the region of a deformed well is taken to be 5 times smaller than the  $\beta$ -vibrational inertia coefficient.

The calculated value of  $\rho^2(0_2^+ \rightarrow 0_1^+)$  is 6 times smaller than the measured value. This indicates a possible influence of the pairing vibrational mode that is not included in the present consideration.

The calculated value of the  $B(M1; 2_2^+ \rightarrow 2_1^+)$  strength demonstrates an excellent agreement with the experimental value. However, this result has been obtained due to using an  $M1$  transition operator that takes into account the result of the shell model for the  $g$  factor of the spherical configuration.

We thank A. Leviatan, V. Werner, and T. Beck for discussions. This work was supported by the German DFG under Grant No. SFB 1245 and by the BMBF under Grant No. 05P19RDFN1.

- 
- [1] J. L. Wood, K. Heyde, W. Nazarewicz, M. Huyse, and P. van Duppen, *Phys. Rep.* **215**, 101 (1992).  
[2] P. Cejnar, J. Jolie, and R. F. Casten, *Rev. Mod. Phys.* **82**, 2155 (2010).  
[3] K. Heyde and J. L. Wood, *Rev. Mod. Phys.* **83**, 1467 (2011); **83**, 1655(E) (2011).  
[4] A. Chakraborty *et al.*, *Phys. Rev. Lett.* **110**, 022504 (2013).  
[5] T. Togashi, Yu. Tsunoda, T. Otsuka, and N. Shimizu, *Phys. Rev. Lett.* **117**, 172502 (2016).  
[6] A. Bohr, *Dan. Mat.-Fys. Medd.* **26**, 1 (1952).  
[7] Z. P. Li, T. Niksić, and D. Vretenar, *J. Phys. G: Nucl. Part. Phys.* **43**, 024005 (2016).  
[8] E. Cheifetz, R. C. Jared, S. G. Thompson, and J. B. Wilhelmy, *Phys. Rev. Lett.* **25**, 38 (1970).  
[9] P. Federman and S. Pittel, *Phys. Lett. B* **77**, 29 (1978).  
[10] P. Federman and S. Pittel, *Phys. Rev. C* **20**, 820 (1979).  
[11] K. Sieja, F. Nowacki, K. Langanke, and G. Martínez-Pinedo, *Phys. Rev. C* **79**, 064310 (2009); **80**, 019905(E) (2009).  
[12] J. E. Garcia-Ramos, K. Heyde, R. Fossion, V. Hellemans, and S. De Baerdemacker, *Eur. Phys. J. A* **26**, 221 (2005).  
[13] M. Büyükkata, P. Van Isacker, and I. Uluer, *J. Phys. G: Nucl. Part. Phys.* **37**, 105102 (2010).  
[14] Y.-X. Liu, Y. Sun, X.-H. Zhou, Y.-H. Zhang, S.-Y. Yu, Y.-C. Yang, and H. Jin, *Nucl. Phys. A* **858**, 11 (2011).  
[15] A. Petrovici, K. W. Schmid, and A. Faessler, *J. Phys.: Conf. Ser.* **312**, 092051 (2011).  
[16] A. Petrovici, *Phys. Rev. C* **85**, 034337 (2012).

- [17] R. Rodríguez-Guzmán, P. Sarriguren, L. M. Robledo, and S. Perez-Martin, *Phys. Lett. B* **691**, 202 (2010).
- [18] J. Skalski, P.-H. Heenen, and P. Bonche, *Nucl. Phys. A* **559**, 221 (1993).
- [19] J. Xiang, Z. P. Li, Z. X. Li, J. M. Yao, and J. Meng, *Nucl. Phys. A* **873**, 1 (2012).
- [20] H. Mei, J. Xiang, J. M. Yao, Z. P. Li, and J. Meng, *Phys. Rev. C* **85**, 034321 (2012).
- [21] J. Skalski, S. Mizutori, and W. Nazarewicz, *Nucl. Phys.* **617**, 282 (1997).
- [22] C. Özen and D. J. Dean, *Phys. Rev. C* **73**, 014302 (2006).
- [23] H. T. Fortune, *Phys. Rev. C* **95**, 054313 (2017).
- [24] N. Gavrielov, A. Leviatan, and F. Iachello (private communication).
- [25] G. Lhersonneau, B. Pfeiffer, K.-L. Kratz, T. Enqvist, P. P. Jauho, A. Jokinen, J. Kantele, M. Leino, J. M. Parmonen, H. Penttilä, and J. Äystö, *Phys. Rev. C* **49**, 1379 (1994).
- [26] M. Büscher, R. F. Casten, R. L. Gill, R. Schuhmann, J. A. Winger, H. Mach, M. Moszyński, and K. Sistemich, *Phys. Rev. C* **41**, 1115 (1990).
- [27] G. Lhersonneau, P. Dendooven, A. Honkanen, M. Huhta, P. M. Jones, R. Julin, S. Juutinen, M. Oinonen, H. Penttilä, J. R. Persson, K. Peräjärvi, A. Savelius, J. C Wang, and J. Äystö, *Phys. Rev. C* **56**, 2445 (1997).
- [28] C. Kremer, S. Aslanidou, S. Bassauer, M. Hilcker, A. Krugmann, P. von Neumann-Cosel, T. Otsuka, N. Pietralla, V. Yu. Ponomarev, N. Shimizu, M. Singer, G. Steinilber, T. Togashi, Y. Tsunoda, V. Werner, and M. Zweidinger, *Phys. Rev. Lett.* **117**, 172503 (2016).
- [29] G. Levai and J. M. Arias, *Phys. Rev. C* **69**, 014304 (2004).
- [30] G. Levai and J. M. Arias, *Phys. Rev. C* **81**, 044304 (2010).
- [31] P. Baganu and R. Budaca, *J. Phys. G: Nucl. Part. Phys.* **42**, 105106 (2015).
- [32] R. Budaca, P. Baganu, and A. I. Budaca, *Phys. Lett. D* **776**, 26 (2018).
- [33] T. Niksić, Z. P. Li, D. Vretenar, L. Próchniak, J. Meng, and P. Ring, *Phys. Rev. C* **79**, 034303 (2009).
- [34] M. A. Caprio, *Phys. Rev. C* **72**, 054323 (2005).
- [35] A. S. Davydov and A. A. Chaban, *Nucl. Phys.* **20**, 499 (1960).
- [36] F. Iachello, *Phys. Rev. Lett.* **87**, 052502 (2001).
- [37] R. V. Jolos and P. von Brentano, *Phys. Rev. C* **76**, 024309 (2007).
- [38] R. V. Jolos and P. von Brentano, *Phys. Rev. C* **77**, 064317 (2008).
- [39] W. Witt, N. Pietralla, V. Werner, and T. Beck (unpublished).
- [40] J. L. Wood, E. F. Zganjar, C. D. Coster, and K. Heyde, *Nucl. Phys. A* **651**, 323 (1999).
- [41] R. V. Jolos and P. von Brentano, *Phys. Rev. C* **79**, 044310 (2009).
- [42] S. Iwasaki, T. Marumori, F. Sakata, and K. Takada, *Prog. Theor. Phys.* **56**, 1140 (1976).
- [43] D. P. Grechukhin, *Nucl. Phys.* **40**, 422 (1963).
- [44] P. Ring and P. Schuck, *The Nuclear Many-Body Problem* (Springer-Verlag, Berlin, 1980).
- [45] N. Yu. Shirikova, R. V. Jolos, N. Pietralla, A. V. Sushkov, and V. V. Voronov, *Eur. Phys. J. A* **41**, 393 (2009).
- [46] O. Prior, F. Boehm, and S. G. Nilsson, *Nucl. Phys. A* **110**, 257 (1968).